

MIT Open Access Articles

Frequency-dependent current noise in quantum heat transfer: A unified polaron calculation

The MIT Faculty has made this article openly available. **Please share** how this access benefits you. Your story matters.

Citation: Liu, Junjie et al. "Frequency-dependent current noise in quantum heat transfer: A unified polaron calculation." The Journal of chemical physics, vol. 148, no. 23, 2018, 234104 © 2018 The Author(s)

As Published: 10.1063/1.5025367

Publisher: AIP Publishing

Persistent URL: <https://hdl.handle.net/1721.1/126060>

Version: Final published version: final published article, as it appeared in a journal, conference proceedings, or other formally published context

Terms of Use: Article is made available in accordance with the publisher's policy and may be subject to US copyright law. Please refer to the publisher's site for terms of use.



Frequency-dependent current noise in quantum heat transfer: A unified polaron calculation

Junjie Liu, Chang-Yu Hsieh, Changqin Wu, and Jianshu Cao

Citation: *The Journal of Chemical Physics* **148**, 234104 (2018); doi: 10.1063/1.5025367

View online: <https://doi.org/10.1063/1.5025367>

View Table of Contents: <http://aip.scitation.org/toc/jcp/148/23>

Published by the [American Institute of Physics](#)

PHYSICS TODAY

WHITEPAPERS

ADVANCED LIGHT CURE ADHESIVES

Take a closer look at what these environmentally friendly adhesive systems can do

READ NOW

PRESENTED BY
 **MASTERBOND**
ADHESIVES | SEALANTS | COATINGS

Frequency-dependent current noise in quantum heat transfer: A unified polaron calculation

Junjie Liu,^{1,2} Chang-Yu Hsieh,^{1,2} Changqin Wu,³ and Jianshu Gao^{1,2}

¹Singapore-MIT Alliance for Research and Technology (SMART) Center, 1 CREATE Way, Singapore 138602, Singapore

²Department of Chemistry, Massachusetts Institute of Technology, 77 Massachusetts Avenue, Cambridge, Massachusetts 02139, USA

³State Key Laboratory of Surface Physics and Department of Physics, Fudan University, Shanghai 200433, China

(Received 9 February 2018; accepted 28 May 2018; published online 20 June 2018)

To investigate frequency-dependent current noise (FDCN) in open quantum systems at steady states, we present a theory which combines Markovian quantum master equations with a finite time full counting statistics. Our formulation of the FDCN generalizes previous zero-frequency expressions and can be viewed as an application of MacDonald's formula for electron transport to heat transfer. As a demonstration, we consider the paradigmatic example of quantum heat transfer in the context of a non-equilibrium spin-boson model. We adopt a recently developed polaron-transformed Redfield equation which allows us to accurately investigate heat transfer with arbitrary system-reservoir coupling strength, arbitrary values of spin bias, and temperature differences. We observe a turn-over of FDCN in the intermediate coupling regimes, similar to the zero-frequency case. We find that the FDCN with varying coupling strengths or bias displays a universal Lorentzian-shape scaling form in the weak coupling regime, and a white noise spectrum emerges with zero bias in the strong coupling regime due to distinctive spin dynamics. We also find that the bias can suppress the FDCN in the strong coupling regime, in contrast to its zero-frequency counterpart which is insensitive to bias changes. Furthermore, we utilize the Saito-Utsumi relation as a benchmark to validate our theory and study the impact of temperature differences at finite frequencies. Together, our results provide detailed dissections of the finite time fluctuation of heat current in open quantum systems. *Published by AIP Publishing.* <https://doi.org/10.1063/1.5025367>

I. INTRODUCTION

The rapid development in nanotechnologies opens an avenue for studying heat transfer in mesoscopic systems.¹⁻⁴ At the nano-scales, fluctuations of heat become increasingly relevant⁵ to the performance and stability of nanostructured devices. To better characterize the fluctuations, higher order statistics of heat transfer beyond the stationary heat current are needed and cannot be directly obtained from the standard heat conductance measurements. Hence, it is desirable to formulate a theoretical framework to analyze heat-transfer statistics for these systems.

So far, analytical results on the heat-transfer statistics are limited to the infinite time limit (i.e., the zero frequency limit) where well-established frameworks such as the large deviation theory,⁶ steady state fluctuation theorem,⁷⁻⁹ and full counting statistics (FCS)¹⁰⁻¹² can be utilized. Both the stationary heat current¹³⁻¹⁵ and variance of heat current have been studied for open quantum systems at steady states.¹⁶⁻²¹ However, this is by no means the complete story. Finite-frequency components of heat fluctuations provide a rich set of new information about the steady state heat statistics beyond what could be inferred from the zero-frequency component, as already demonstrated for electronic heat transport in the wide-band limit.²² Apart from this example, and

some notable exceptions,^{23,24} the behaviors of the finite frequency heat-transfer statistics are still largely unexplored due to the absence of a general theoretical framework that can extract finite time fluctuation properties of heat at steady states.

In this work, we present a theoretical method to study the frequency-dependent current noise (FDCN) for nonequilibrium open quantum systems.²⁵⁻²⁷ We extend MacDonald's formula^{28,29} in electron transport to heat current which formally expresses the FDCN in terms of an integral of the time-dependent second order cumulant of transferred heat evaluated at steady states, thus generalizing previously expressions for zero-frequency heat current noise.¹⁸⁻²¹ In order to calculate the time-dependent cumulant of heat involved in the FDCN, we follow the scheme of a finite time FCS developed for electron transport^{30,31} and propose an analogous framework. Our theory can be applied to open quantum systems described by Markovian quantum master equations and possesses good adaptability. Figure 1 clearly summarizes the physical picture underlying the finite-time heat fluctuation we introduce in the present work.

To illustrate the formalism, we study the case of a nonequilibrium spin-boson (NESB) model^{26,33} which is a paradigmatic example for quantum heat transfer.¹³ By combining a recently developed nonequilibrium polaron-transformed

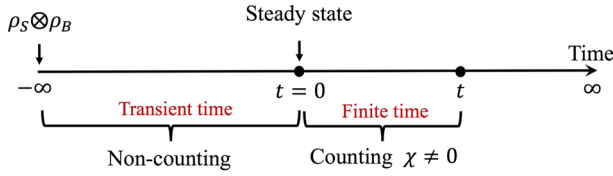


FIG. 1. Illustration of the “finite time” parameter regime. The total system has reached the steady state at $t = 0$. The two-time measurements are taken at $t = 0$ and t with a nonzero counting field χ .

Redfield equation (NE-PTRE) for the reduced spin dynamics^{14,20} and the finite time FCS, we are able to study the FDCN of the NESB from a unified perspective. New phenomena are found and explained analytically. These results manifest the versatility of our proposed framework and how it can be used to study FDCN in a variety of quantum transport setups.^{34–36}

The paper is organized as follows. We first propose our general theory for the FDCN in Sec. II. In Sec. III, we introduce the NESB model and the NE-PTRE with FCS. In Sec. IV, we study the FDCN of the NESB in detail by analyzing the impact of coupling strength, bias, and temperature differences. In Sec. V, we summarize our findings.

II. THEORY

A. Frequency-dependent heat current noise power

We consider heat transfer systems, consisting of a central region attached to non-interacting bosonic reservoirs at *different temperatures*. This setup can be described by a general Hamiltonian

$$H = H_s + H_I + H_B, \quad (1)$$

where H_s refers to the system, $H_B = \sum_{v=L,R} H_B^v = \sum_{k,v=L,R} \omega_{k,v} b_{k,v}^\dagger b_{k,v}$ is the bosonic reservoirs' part with $b_{k,v}^\dagger$ and $b_{k,v}$ being the bosonic creation and annihilation operators for the mode k of frequency $\omega_{k,v}$ in the v th reservoir characterized by an inverse temperature $\beta_v \equiv T_v^{-1}$ ($T_L \neq T_R$), $H_I = \sum_v V_v \otimes B_v$ is the interaction between the system and reservoirs which assumes a bilinear form with B_v being an arbitrary operator of the v th reservoir and V_v being the corresponding system operator. This setup encompasses a broad range of dissipative and transport settings. Throughout the paper, we set $\hbar = 1$ and $k_B = 1$.

The stationary heat current is defined by

$$\langle I_v(t) \rangle = -\frac{d}{dt} \langle H_B^v(t) \rangle, \quad (2)$$

where we denote $\langle \cdots \rangle \equiv \text{Tr}[\cdots \rho_{ss}]$ with ρ_{ss} being the total steady state density matrix. Due to the energy conservation, we introduce $\langle I \rangle \equiv \langle I_L \rangle = -\langle I_R \rangle$. We simply focus on the heat current I and its fluctuation statistics. It is worthwhile to mention that the above definition is consistent with the quantum thermodynamics and can be applied in the strong coupling regime.³⁷

We assume that the total system has reached the unique steady state at $t = 0$ and then the heat current noise at finite times is described by the symmetrized auto-correlation

function²²

$$S(t_1, t_2) = \frac{1}{2} \langle \{ \Delta I(t_1), \Delta I(t_2) \} \rangle \quad (3)$$

with $\Delta I(s) = I(s) - \langle I \rangle$ being the fluctuation of time dependent heat current $I(s) = -\frac{d}{ds} H_B^L(s)$ from its average value, where the anti-commutator $\{A, B\} = AB + BA$ ensures the Hermitian property. At steady states, the correlation function only depends on the time difference such that $S(t_1, t_2) = S(\tau)$ with $\tau = |t_1 - t_2|$ being the time interval. Therefore, the Fourier transform yields the FDCN $S(\omega)$ for the heat current

$$S(\omega) = S(-\omega) = \int_{-\infty}^{\infty} d\tau e^{i\omega\tau} S(\tau) \geq 0. \quad (4)$$

Since $S(\omega)$ is an even function in frequency and strictly semi-positive in accordance with the Wiener-Khintchine theorem, in the following we consider positive values of the frequency, $\omega > 0$, only.

According to the definition of heat current in Eq. (2), we can introduce $Q(t) = H_B^L(t) - H_B^L(0)$ as the heat transferred from the left reservoir to the right reservoir in the time span 0 to t ¹² [we assume that the left reservoir has a higher temperature and $H_B^L(t)$ is the Hamiltonian operator in the Heisenberg picture] with $\langle Q(t) \rangle = \langle I \rangle t$, and in analogy with MacDonald's formula in electron charge transport,^{28,29} we find (for completeness, we present a derivation for heat transfer in the Appendix)

$$S(\omega) = \omega \int_0^{\infty} dt \sin(\omega t) \frac{\partial}{\partial t} \langle Q^2(t) \rangle_c, \quad (5)$$

where we define the second order cumulant of heat as $\langle Q^2(t) \rangle_c \equiv \langle Q^2(t) \rangle - \langle Q(t) \rangle^2$. Equation (5) can be viewed as an application of MacDonald's formula in electron charge transport to heat transfer. However, in contrast to the electron charge current, the above MacDonald-like formula represents the total heat current noise spectrum due to the absence of a displacement current component in heat transfer setups. This formally exact relation enables us to calculate FDCN from the finite time heat statistics. The second order cumulant involved in the above definition can be obtained from the cumulant generating function (CGF) which is the main focus of the FCS (see, e.g., Ref. 8 and reference therein). However, instead of considering the FCS in the infinite time limit as in previous heat transfer studies, we should follow the framework of a finite time FCS developed for electron transport^{30,31} such that finite time properties of cumulants of transferred heat which are essential for the finite-frequency noise power can be extracted.

The above finite frequency definition for $S(\omega)$ can recover the well-known zero-frequency expression. To see this, we introduce the regularization³⁸

$$\omega \sin \omega t = (\omega \sin \omega t + \varepsilon \cos \omega t) e^{-\varepsilon t}, \quad \varepsilon \rightarrow 0^+, \quad (6)$$

which ensures correct results at the $\omega = 0$ case. Then Eq. (5) reduces to

$$S(0) = \varepsilon \int_0^{\infty} e^{-\varepsilon t} \frac{\partial}{\partial t} \langle Q^2(t) \rangle_c \Big|_{\varepsilon \rightarrow 0^+}. \quad (7)$$

By using the final value theorem of the Laplace transform, we obtain

$$S(0) = \frac{\partial}{\partial t} \langle Q^2(t) \rangle_c \Big|_{t \rightarrow \infty}. \quad (8)$$

In the infinite time limit (see Fig. 1), all cumulants increase linearly in time t as guaranteed by the FCS,⁸ then the above relation is just the expression utilized in recent studies on $S(0)$.^{18–21} Therefore, Eq. (5) generalizes previous zero-frequency expressions.

B. Finite time full counting statistics

1. Finite time generating functions

In accordance with the definition of heat current, we study the statistics of heat $Q(t)$ transferred from the left reservoir to the right reservoir during a time interval $[0, t]$. The specific measurement of the net transferred heat $Q(t)$ is performed using a two-time measurement protocol:^{8,39} Initially at time $t = 0$ where the total system has reached the steady state, we introduce a projector $K_{q_0} = |q_0\rangle\langle q_0|$ with $|q_0\rangle$ being one of the eigen-states of the left bath Hamiltonian H_B^L to measure the quantity H_B^L , giving an outcome q_0 . A second measurement is performed at time t with a projector $K_{q_t} = |q_t\rangle\langle q_t|$ ($|q_t\rangle$ is also one of the eigen-states of the left bath Hamiltonian H_B^L at time t) and an outcome q_t . Hence, the measurement outcome of net transferred heat is determined by $Q(t) = q_t - q_0$. The corresponding joint probability to measure q_0 at $t = 0$ and q_t at time t reads

$$P[q_t, q_0] \equiv \text{Tr}\{K_{q_t} U(t, 0) K_{q_0} \rho(0) K_{q_0} U^\dagger(t, 0) K_{q_t}\}, \quad (9)$$

where $U(t, 0)$ is the unitary time evolution operator of the total system and $\rho(0)$ is the total density matrix when the counting starts. We should choose $\rho(0) = \rho_{ss}$ as we are interested in fluctuations at steady states. Such an initial condition can be constructed by switching on the interaction H_I from the infinite past, where the density matrix $\rho(-\infty)$ is given by a direct product of density matrices of the system ρ_s and bosonic baths ρ_B . The corresponding counting scheme is illustrated in Fig. 1. The probability distribution for the difference $Q(t) = q_t - q_0$ between the outputs of the two measurements is given by

$$p(Q, t) = \sum_{q_t, q_0} \delta[Q(t) - (q_t - q_0)] P[q_t, q_0], \quad (10)$$

where $\delta(x)$ denotes the Dirac distribution. Then we can introduce a finite time moment generating function (MGF) associated with this probability,

$$Z(\chi, t) = \int dQ(t) p(Q, t) e^{i\chi Q(t)} \quad (11)$$

with χ being the counting-field parameter. Its logarithm gives the CGF $G(\chi, t) = \ln Z(\chi, t)$.

To derive explicit expressions for generating functions that are suitable for analytical as well as numerical studies, we focus on open quantum systems described by a reduced density matrix $\rho_s(t)$ which obeys a generalized Markovian master equation

$$\dot{\rho}_s(t) = -L\rho_s(t) \quad (12)$$

with $\dot{A}(t) \equiv \frac{\partial A(t)}{\partial t}$ and L being the Liouvillian operator driving the dynamics of the system. Although we limit ourselves to Markovian master equations, an extension to include non-Markovian effects^{40–42} is possible, which will be addressed in the future work.

In order to investigate the statistics of transferred heat during the time span $[0, t]$ at steady states, we proceed by projecting the reduced density matrix $\rho_s(t)$ onto the subspace of Q net transferred heat and denote this Q -resolved density matrix as $\rho_s(Q, t)$, in analogy with the n -resolved density matrix in quantum optics⁴³ and mesoscopic electron transport.⁴⁴ The probability $p(Q, t)$ in Eq. (10) is just

$$p(Q, t) = \text{Tr}[\rho_s(Q, t)]. \quad (13)$$

The MGF can conveniently be expressed as

$$Z(\chi, t) = \text{Tr}[\rho_s(\chi, t)] \quad (14)$$

in terms of the χ -dependent density matrix $\rho_s(\chi, t) = \int dQ e^{i\chi Q} \rho_s(Q, t)$. We note that by setting $\chi = 0$, we recover the original density matrix: $\rho_s(\chi = 0, t) = \rho_s(t)$.

To evaluate the MGF and CGF, we consider a modified master equation governing the evolution of the χ -dependent master matrix. According to Eq. (12), the modified master equation takes the form of

$$\dot{\rho}_s(\chi, t) = -L_\chi \rho_s(\chi, t) \quad (15)$$

with a χ -dependent Liouvillian L_χ . Since Eq. (15) is a linear differential equation for $\rho_s(\chi, t)$, it can be rewritten as

$$|\dot{\rho}_s(\chi, t)\rangle\rangle = -\mathbb{L}_\chi |\rho_s(\chi, t)\rangle\rangle, \quad (16)$$

where $|\rho_s(\chi, t)\rangle\rangle$ is the vector representation of $\rho_s(\chi, t)$ and \mathbb{L}_χ is the matrix representation of L_χ in the Liouville space.⁸ Here we use double angle brackets to distinguish these vectors from the ordinary quantum mechanical “bras” and “kets.” By formally solving the above equation, we find

$$|\rho_s(\chi, t)\rangle\rangle = e^{-\mathbb{L}_\chi t} |\rho_s^{stat}\rangle\rangle, \quad (17)$$

as we require that the system at $t = 0$ has reached the steady state defined by $\mathbb{L}|\rho_s^{stat}\rangle\rangle = 0$ or by simply tracing out the reservoir degrees of freedom in the total steady state ρ_{ss} . Since the Liouvillian L conserves probability, it holds that $\text{Tr}[L\rho_s(t)] = 0$ for any density matrix. This implies that the left zero-eigenvector of \mathbb{L} is the vector representation of the trace operation, i.e., $\langle\langle \tilde{0} | \mathbb{L} = 0$ and $\langle\langle \tilde{0} | \rho_s^{stat}\rangle\rangle = \text{Tr}[\rho_s^{stat}] = 1$. Combining Eqs. (14) and (17), we then obtain the following compact expression:

$$Z(\chi, t) = \langle\langle \tilde{0} | e^{-\mathbb{L}_\chi t} |\rho_s^{stat}\rangle\rangle \equiv \langle\langle e^{-\mathbb{L}_\chi t} \rangle\rangle, \quad (18)$$

which holds for a system that has been prepared in an arbitrary state in the distant past. The system has then evolved until $t = 0$, where it has reached the steady state. At $t = 0$, we start collecting statistics to construct the probability distribution $p(Q, t)$ for Q net transferred heat in the time span $[0, t]$.

We then diagonalize the \mathbb{L}_χ as

$$\mathbb{L}_\chi = \sum_n \mu_n(\chi) |f_n(\chi)\rangle\rangle \langle\langle g_n(\chi) | \quad (19)$$

with μ_n being the n th eigenvalue and $|f_n(\chi)\rangle\rangle$ and $\langle\langle g_n(\chi)|$ being the corresponding right and left eigenvectors, respectively. In the $\chi \rightarrow 0$ limit, one of these eigenvalues, say $\mu_0(\chi)$, tends to zero and the corresponding eigenvectors give the stationary states $\langle\langle \tilde{0}|$ and $|\rho_s^{stat}\rangle\rangle$ for the system. This single eigenvalue is sufficient to determine the zero-frequency FCS.¹¹ By contrast, here we need all eigenvalues and eigenvectors for constructing finite time FCS. We can rewrite the MGF as

$$Z(\chi, t) = \sum_n e^{-\mu_n(\chi)t} F_n(\chi) \quad (20)$$

with $F_n(\chi) = \langle\langle \tilde{0}|f_n(\chi)\rangle\rangle \langle\langle g_n(\chi)|\rho_s^{stat}\rangle\rangle$. Consequently, the CGF can be expressed as $G(\chi, t) = \ln \sum_n e^{-\mu_n(\chi)t} F_n(\chi)$.

2. Expressions of FDCN

Introducing the n th cumulant $\langle Q^n(t) \rangle_c$ of $Q(t)$ as

$$\langle Q^n(t) \rangle_c = \left. \frac{\partial^n}{\partial (i\chi)^n} G(\chi, t) \right|_{\chi=0}, \quad (21)$$

and the coefficients

$$C_m^n(t) = \left. \frac{\partial^{n+m}}{\partial (i\chi)^n \partial A^m} G(\chi, t) \right|_{\chi=0}, \quad (22)$$

where $A \equiv \beta_R - \beta_L$ denotes the affinity, we will have

$$S(\omega) = \omega \int_0^\infty dt \sin \omega t \frac{\partial}{\partial t} C_0^2(t). \quad (23)$$

This formal exact relation represents a nonlinear superposition of thermal (Johnson-Nyquist), shot, and quantum noises and enables us to investigate the FDCN within the framework of finite time FCS for open quantum systems, thus constituting one of main results in this work. If we introduce J_m^n as the long time limit of $\frac{\partial}{\partial t} C_m^n(t)$, then $S(0) = J_0^2$ according to Eq. (8).

Equation (23) is particularly useful in obtaining analytical results provided that the dimension of the Liouvillian operator \mathbb{L}_χ is relatively small. If the eigen-problem of the Liouvillian operator becomes complicated, we should resort to a numerical treatment. We note

$$C_0^2(t) = \langle Q^2(t) \rangle - \langle Q(t) \rangle^2 = \langle Q^2(t) \rangle - (It)^2 \quad (24)$$

in steady states with $\langle Q^2(t) \rangle$ being the second order moment of heat $Q(t)$ generated by the MGF: $\frac{\partial^2}{\partial (i\chi)^2} Z(\chi, t)|_{\chi=0}$. Inserting this expression into Eq. (23) and evaluating the integral, we have

$$S(\omega) = \omega \frac{\partial^2}{\partial (i\chi)^2} \int_0^\infty dt \sin \omega t \frac{\partial}{\partial t} Z(\chi, t)|_{\chi=0}. \quad (25)$$

Utilizing the Laplace transform ($t \rightarrow \lambda$), the above equation can be cast into⁴¹

$$S(\omega) = -\frac{\omega^2}{2} \frac{\partial^2}{\partial (i\chi)^2} [\langle\langle \Omega(\chi, \lambda = i\omega) + \Omega(\chi, \lambda = -i\omega) \rangle\rangle] |_{\chi=0}, \quad (26)$$

where we denote $Z(\chi, \lambda) = \langle\langle \Omega(\chi, \lambda) \rangle\rangle$ with $\Omega(\chi, \lambda) = (\lambda + \mathbb{L}_\chi)^{-1}$. This expression is more suitable for numerical simulations as only the stationary state at $t = 0$ and the Liouvillian operator are needed.

III. NONEQUILIBRIUM SPIN-BOSON MODEL

A. Model setup

To illustrate our general method, we analyze the statistics of the prototypical example of quantum heat transfer through a NESB model.^{26,33} The NESB consists of a two-level spin in the central region and is described by the Hamiltonian

$$H_s = \frac{\varepsilon_0}{2} \sigma_z + \frac{\Delta}{2} \sigma_x, \quad (27)$$

where ε_0 is the bias, Δ is the tunnelling constant between two levels, and $\sigma_{x,z}$ are the Pauli matrices. Since the spectrum of the system Hamiltonian is a symmetric function of bias, here we only consider positive bias. The operators in the interaction term H_I read

$$V_v = \sigma_z, \quad B_v = \sum_k g_{k,v} (b_{k,v}^\dagger + b_{k,v}) \quad (28)$$

with $g_{k,v}$ being the system-reservoir coupling strength. The influence of bosonic reservoirs is characterized by a spectral density $\gamma_v(\omega) = 2\pi \sum_k g_{k,v}^2 \delta(\omega - \omega_{k,v})$. For reservoirs with infinite degrees of freedom, $\gamma_v(\omega)$ can be regarded as a continuous function of its argument; then, we can let $\gamma_v(\omega) = \pi \alpha_v \omega^s \omega_{c,v}^{1-s} e^{-\omega/\omega_{c,v}}$ with α_v being the dimensionless system-reservoir coupling strength of the order of $g_{k,v}^2$ and $\omega_{c,v}$ being the cut-off frequency of the v th bosonic reservoir. For simplicity and without loss of generality, we consider the super-Ohmic spectrum $s = 3$ which is of experimental relevance⁴⁵ and choose $\alpha_L = \alpha_R = \alpha$, $\omega_{c,L} = \omega_{c,R} = \omega_c$.

We limit our calculation to the so-called nonadiabatic limit of $\Delta/\omega_c \ll 1$. For fast reservoirs, it has been demonstrated that the polaron transformation (PT) is suitable for the entire range of system-bath coupling strength^{14,15,46,47} and enables us to study the impact of system-reservoir interaction beyond the weak coupling limit. Thus we perform the PT with the unitary operator

$$U = \exp[i\sigma_z \Phi/2], \quad \Phi = 2i \sum_{k,v} \frac{g_{k,v}}{\omega_{k,v}} (b_{k,v}^\dagger - b_{k,v}) \quad (29)$$

such that

$$H_T = U^\dagger H U = \tilde{H}_0 + \tilde{H}_I, \quad (30)$$

where the free Hamiltonian is $\tilde{H}_0 = \tilde{H}_s + \tilde{H}_B$ with the reservoir Hamiltonian remains unaffected, $\tilde{H}_B = H_B$, and the transformed system Hamiltonian reads

$$\tilde{H}_s = \frac{\varepsilon_0}{2} \sigma_z + \frac{\eta \Delta}{2} \sigma_x, \quad (31)$$

where the renormalization factor due to the formation of polarons reads^{14,20,48,49}

$$\eta = \exp\left(-\sum_v \int_0^\infty d\omega \frac{\gamma_v(\omega)}{2\pi\omega^2} \coth \frac{\beta_v \omega}{2}\right). \quad (32)$$

For the super-Ohmic spectrum $s = 3$ we consider here, the renormalization factor is specified as $\eta = \exp\{-\sum_v \alpha[-1 + \frac{2}{(\beta_v \omega_c)^2} \psi_1(1/\beta_v \omega_c)]/2\}$, with the trigamma function $\psi_1(x) = \sum_{n=0}^{\infty} 1/(n+x)^2$. As can be seen, in the weak coupling regime, η becomes 1, while in the strong coupling regime, it vanishes. The transformed interaction term, originated from the tunneling term in Eq. (27), takes the following form:

$$\tilde{H}_I = \frac{\Delta}{2} [\sigma_x (\cos \Phi - \eta) + \sigma_y \sin \Phi]. \quad (33)$$

It's evident that \tilde{H}_I contains arbitrary orders of the system-reservoir coupling strength by noting the form of Φ in Eq. (29); however, its average vanishes. Hence we can treat \tilde{H}_I perturbatively, regardless of the coupling strength. Therefore, in the polaron picture, we can study finite time FCS from the weak to strong system-reservoir coupling regime.

B. Nonequilibrium polaron-transformed redfield equation

In order to study finite time FCS of heat in the polaron picture, we follow a recently developed NE-PTRE method which leads to the following master equation for the reduced density matrix $\rho_s(t)$:^{14,20}

$$\dot{\rho}_s(t) = -i[\tilde{H}_s, \rho_s] + \sum_{l=e,o} \sum_{\omega, \omega'=\pm\omega_0} \Gamma_l(\omega) [P_l(\omega) \rho_s, P_l(\omega')] + \text{H.c.}, \quad (34)$$

where $\omega_0 = \sqrt{\varepsilon_0^2 + \eta^2 \Delta^2}$ is the energy gap in the eigenbasis and $P_{e(o)}(\omega)$ is the transition projector in the eigenbasis obtained from the evolution of Pauli matrices $\sigma_{x(y)}(-\tau) = \sum_{\omega=0, \pm\omega_0} P_{e(o)} e^{i\omega\tau}$. The subscript $e(o)$ denotes the even (odd) parity of the transfer dynamics. The transition rates are $\Gamma_o(\omega) = \left(\frac{\eta\Delta}{2}\right)^2 \int_0^\infty d\tau e^{i\omega\tau} \sinh[Q_c(\tau)]$ and $\Gamma_e(\omega) = \left(\frac{\eta\Delta}{2}\right)^2 \int_0^\infty d\tau e^{i\omega\tau} (\cosh[Q_c(\tau)] - 1)$ with $Q_c(\tau)$ denoting the sum of bosonic correlation functions $Q_c(\tau) = \sum_v Q_v(\tau)$,

$$Q_v(\tau) = \int_0^\infty d\omega \frac{\gamma_v(\omega)}{\pi\omega^2} \left[\coth \frac{\beta_v \omega}{2} \cos \omega\tau - i \sin \omega\tau \right]. \quad (35)$$

As clearly demonstrated in Ref. 20, $\Gamma_{o(e)}(\omega)$ describe totally different transfer processes.

Combining Eq. (34) with a counting field χ , we have the following χ -dependent NE-PTRE for the χ -dependent density matrix²⁰

$$\dot{\rho}_s(\chi, t) = -i[\tilde{H}_s, \rho_s(\chi, t)] + \mathcal{D}_\chi[\rho_s(\chi, t)], \quad (36)$$

where the dissipator reads $\mathcal{D}_\chi[\rho_s] = \sum_l \sum_{\omega, \omega'} \{[\Gamma_{l,-}^X(\omega) + \Gamma_{l,+}^X(\omega')] P_l(\omega') \rho_s P_l(\omega) - [\Gamma_{l,+}(\omega) P_l(\omega') P_l(\omega) \rho_s + \text{H.c.}]\}$ and χ -dependent transition rates are expressed as ($\sigma = \pm$),

$$\begin{aligned} \Gamma_{e,\sigma}^X(\omega) &= \left(\frac{\eta\Delta}{2}\right)^2 \int_0^\infty d\tau e^{i\omega\tau} [\cosh Q_c(\tau_\sigma^X) - 1], \\ \Gamma_{o,\sigma}^X(\omega) &= \left(\frac{\eta\Delta}{2}\right)^2 \int_0^\infty d\tau e^{i\omega\tau} \sinh Q_c(\tau_\sigma^X), \end{aligned} \quad (37)$$

where $\tau_\sigma^X \equiv \sigma\tau - \chi$ and the χ -dependent bosonic correlation function becomes $Q_c(\tau - \chi) = Q_L(\tau - \chi) + Q_R(\tau)$. We note that the NE-PTRE¹⁴ provides an accurate account of the nonequilibrium response of a quantum system contacted by super-Ohmic bath models in the scaling and high-temperature limits such that the Markovian approximation holds.

Defining the vector form of the χ -dependent reduced density matrix as $|\rho_s(\chi, t)\rangle\rangle = [P_{11}^X, P_{00}^X, P_{10}^X, P_{01}^X]^T$ with $P_{ij}^X = \langle i|\rho_s(\chi, t)|j\rangle$, we can express the χ -dependent NE-PTRE in the Liouville space, i.e., $|\dot{\rho}_s(\chi, t)\rangle\rangle = -\mathbb{L}_\chi |\rho_s(\chi, t)\rangle\rangle$. Inserting the form of \mathbb{L}_χ obtained from the χ -dependent NE-PTRE Eq. (36) into the formal expression for $S(\omega)$ Eq. (26), we can obtain explicit numerical results for the FDCN as a function of coupling strength, bias, and temperature differences. In the following section (i.e. Sec. IV), we will provide detailed results.

IV. RESULTS

A. Effect of coupling strength

We first investigate the behaviors of $S(\omega)$ with varying system-reservoir coupling strength under the condition of fixed temperatures and zero bias. Typical numerical results are shown in Fig. 2. We find that even at finite frequencies, the noise spectrum still depicts a non-monotonic turnover behavior in the intermediate coupling regime as that in the zero-frequency case.²⁰ Another interesting finding is that $S(\omega)$ has distinct frequency dependences in the weak and strong coupling regimes (details are listed in Fig. 3): In the weak coupling regime, $S(\omega)$ is a monotonic increasing function of ω and saturates at high frequency [Fig. 3(a)]. The inset further shows that all the data with varying coupling strengths collapse on to one curve, implying the emergence of a universal scaling whose analytical form will be given below. In the strong coupling regime, $S(\omega)$ simply follows a white noise spectrum over the entire frequency range [Fig. 3(b)]. In order to understand such distinct behaviors, we note that the NE-PTRE reduces to the conventional quantum

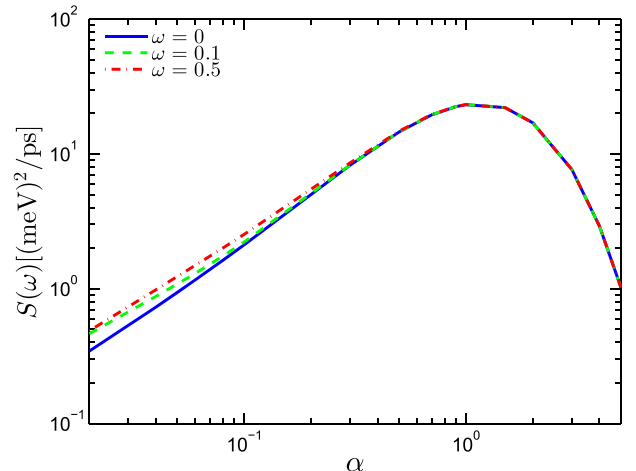


FIG. 2. Behaviors of noise spectrum $S(\omega)$ with varying system-reservoir coupling strength α for different frequencies. Other parameters are $\Delta = 5.22$ meV, $\omega_c = 26.1$ meV, $\varepsilon_0 = 0$, $T_L = 180$ K, and $T_R = 90$ K.

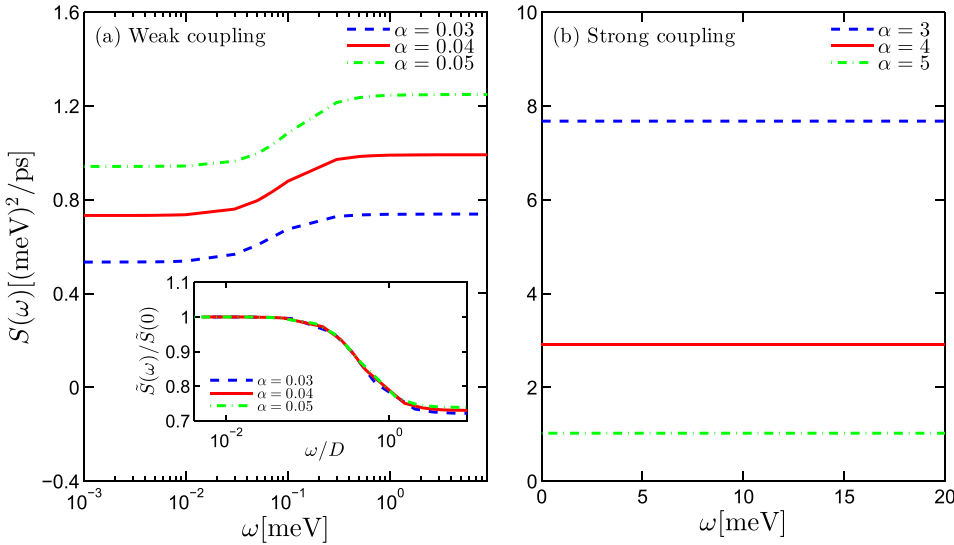


FIG. 3. Behaviors of noise spectrum $S(\omega)$ as a function of ω with varying coupling strength α for (a) weak couplings and (b) strong couplings. The inset in (a) shows universal behaviors of a scaled noise power $\tilde{S}(\omega)$ [defined in Eq. (43)] in the weak coupling regime; the scale parameter D is the sum of total relaxation and activation rates in the Redfield picture. Other parameters are $\Delta = 5.22$ meV, $\omega_c = 26.1$ meV, $\varepsilon_0 = 0$ meV, $T_L = 180$ K, and $T_R = 90$ K.

Redfield master equation (RME) and nonequilibrium non-interacting blip approximation (NE-NIBA) in the weak and strong coupling regimes, respectively.^{14,20,35} Thus we focus on these two limits and present analytical analyses in the following.

1. Weak coupling regime

We first concentrate on the weak coupling case and consider the RME for the reduced dynamics^{48,50} (see the schematic picture in Fig. 4). We denote the relaxation and activation rates due to the v th reservoir as

$$k_{1 \rightarrow 0}^v = \gamma_v(\Delta)[1 + n_v(\Delta)], \quad k_{0 \rightarrow 1}^v \equiv k_{1 \rightarrow 0}^v e^{-\beta_v \Delta}, \quad (38)$$

respectively, where γ_v and n_v are the spectral density and Bose-Einstein distribution of v th bath, respectively. Introducing p_n ($n = 0, 1$) as the probability of the spin system to occupy the state $|n\rangle$, satisfying $p_0(t) + p_1(t) = 1$, then we have

$$|\dot{\rho}_s(t)\rangle\rangle = -\begin{pmatrix} k_d & -k_u \\ -k_d & k_u \end{pmatrix} |\rho_s(t)\rangle\rangle = -\mathbb{L}^R |\rho_s(t)\rangle\rangle, \quad (39)$$

where $|\rho_s(t)\rangle\rangle = (p_1, p_0)^T$ and the total activation and relaxation rates read

$$k_u = \sum_v k_{0 \rightarrow 1}^v, \quad k_d = \sum_v k_{1 \rightarrow 0}^v, \quad (40)$$

respectively. From the above rate equation, the stationary state solution corresponds to $|\rho_s^{stat}\rangle\rangle = \frac{1}{k_d + k_u} (k_u, k_d)^T$ which is just the right zero-eigenvector of \mathbb{L}^R , and the corresponding left zero-eigenvector reads $\langle\langle \tilde{0} | = (1, 1)$ such that $\langle\langle \tilde{0} | \rho_s^{stat}\rangle\rangle = 1$.

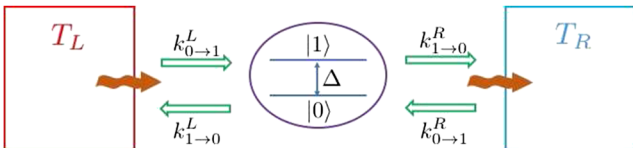


FIG. 4. Schematic picture for the nonequilibrium spin-boson model in the Redfield master equation framework.

To study the statistics of heat, we split $p(Q, t)$ [Eq. (10)] into two part, namely, $p(Q, t) = p_0(Q, t) + p_1(Q, t)$, where $p_0(Q, t)$ denotes the probability transferring heat Q from the left reservoir into the right reservoir, within time interval $[0, t]$, with the spin on the $|0\rangle$ energy level at time t (the counting begins at $t = 0$), and $p_1(Q, t)$ is defined similarly with the spin on the $|1\rangle$ energy level instead. By applying the transformation $p_n(\chi, t) = \int dQ p_n(Q, t) e^{i\chi Q}$, we find

$$|\dot{\rho}_s(\chi, t)\rangle\rangle = -\begin{pmatrix} k_d & -\tilde{k}_u \\ -\tilde{k}_d & k_u \end{pmatrix} |\rho_s(\chi, t)\rangle\rangle = -\mathbb{L}_\chi^R |\rho_s(\chi, t)\rangle\rangle \quad (41)$$

with $|\rho_s(\chi, t)\rangle\rangle = (p_1(\chi, t), p_0(\chi, t))^T$, $\tilde{k}_d = k_{1 \rightarrow 0}^L e^{i\chi \Delta} + k_{1 \rightarrow 0}^R$, and $\tilde{k}_u = k_{0 \rightarrow 1}^L e^{-i\chi \Delta} + k_{0 \rightarrow 1}^R$. A cumbersome evaluation within the Redfield picture yields the following, nontrivial explicit expression for $S(\omega)$ valid in the weak coupling regime:

$$\frac{S(\omega)}{\Delta^2} = R - \frac{2k_L^2}{[D(\omega^2 + D^2)]} [D^2 e^{-\beta_L \Delta} + (k_u - k_d e^{-\beta_L \Delta})^2], \quad (42)$$

where $D = k_d + k_u$ is the sum of total relaxation and activation rates and $R = (k_u k_L + k_d k_L e^{-\beta_L \Delta})/D = p_1^{ss} k_{1 \rightarrow 0}^L + p_0^{ss} k_{0 \rightarrow 1}^L$ is the dynamical activity,^{51,52} which is the average number of transitions per time induced by the left reservoir. From the above equation, we see that $S(\omega)$ increases from $S(0)$ as ω increases and finally saturates at the value determined by the dynamical activity R , in accordance with numerical results shown in Fig. 3(a). If we define a scaled FDCN

$$\tilde{S}(\omega) \equiv R \Delta^2 - S(\omega), \quad (43)$$

a direct consequence of Eq. (42) is that $\tilde{S}(\omega)$ has a universal scaling expression

$$\frac{\tilde{S}(\omega)}{\tilde{S}(0)} = \mathcal{P}(\omega/D) \quad (44)$$

with the scaling function \mathcal{P} endowing a Lorentzian shape and approaching 1 as $\omega \rightarrow 0$. This universal behavior is manifested in our numerical results as can be seen from the inset in Fig. 3(a).

It would be interesting to see whether a similar scaling form in the weak coupling regime holds beyond the NESB model. For multi-level systems, the rates are still proportional to the coupling strength α in the weak coupling regime; we then expect a scaling function $\mathcal{F}(\omega/\alpha)$ still exists; however, the existence of multiple time scales will result in a complicated functional form of \mathcal{F} . Only for systems with a single time scale, as Eq. (42) shows, the function \mathcal{F} endows a Lorentzian shape.

2. Strong coupling regime

We next turn to the white noise spectrum in the strong coupling regime, where the NE-PTRE is consistent with the NE-NIBA framework.^{14,20} Using the NE-NIBA, the population dynamics with zero bias satisfies^{18,19,49}

$$|\dot{\rho}_s(t)\rangle\rangle = -\begin{pmatrix} K & -K \\ -K & K \end{pmatrix} |\rho_s(t)\rangle\rangle = -\mathbb{L}^N |\rho_s(t)\rangle\rangle, \quad (45)$$

where the transition rate K is given by^{14,20}

$$K = (\eta\Delta/2)^2 \int_{-\infty}^{\infty} dt e^{Q_L(t)+Q_R(t)}. \quad (46)$$

From the equation of motion, the stationary state can be obtained as

$$\langle\langle \tilde{0} | \rangle\rangle = \frac{1}{2}(1, 1, \quad |\rho_s^{stat}\rangle\rangle) = (1, 1)^T. \quad (47)$$

In contrast to Eq. (39) of RME, now the diagonal and off-diagonal elements of \mathbb{L}^N are equal. As can be seen in the following, this distinctive spin dynamics with a single transition rate leads to the white noise we observed in Fig. 3(b).

By incorporating the counting field, the equation of motion, Eq. (45), becomes

$$\begin{aligned} |\dot{\rho}_s(\chi, t)\rangle\rangle &= -\begin{pmatrix} K & -K_\chi \\ -K_\chi & K \end{pmatrix} |\rho_s(\chi, t)\rangle\rangle \\ &= -\mathbb{L}_\chi^N |\rho_s(\chi, t)\rangle\rangle \end{aligned} \quad (48)$$

with the χ -dependent transition rate $K_\chi = (\eta\Delta/2)^2 \int_{-\infty}^{\infty} dt e^{Q_L(t-\chi)+Q_R(t)}$.^{14,20} According to Eq. (26), after some algebras, we find

$$S(\omega) = \frac{\partial^2}{\partial(i\chi)^2} K_\chi \Big|_{\chi=0}, \quad (49)$$

which is just $S(0)$ by definition; thus, we demonstrate that $S(\omega)$ is indeed a white noise spectrum and confirms our finding in the strong coupling regime as Fig. 3(b) shows.

To gain more insights, we look at the explicit expression for the MGF. By diagonalizing the matrix \mathbb{L}_χ^N , we find eigenvalues $\mu_0(\chi) = K - K_\chi$ and $\mu_1(\chi) = K + K_\chi$ and the corresponding eigenvectors read $\langle\langle g_n(\chi) | \rangle\rangle = \frac{(K_\chi - K - \mu_n(\chi))}{K_\chi^2 + (K - \mu_n(\chi))^2}$ and $|f_n(\chi)\rangle\rangle = (K_\chi, K - \mu_n(\chi))^T$ with $n = 0, 1$. It is evident that $\langle\langle g_1(\chi) | \rho_s^{stat}\rangle\rangle = \langle\langle \tilde{0} | f_1(\chi)\rangle\rangle = 0$, then we find from Eq. (20) that

$$Z(\chi, t) = e^{-\mu_0(\chi)t}, \quad (50)$$

which is exactly the MGF obtained in the infinite time limit,^{18,49} thus we should have $S(\omega) = S(0)$ in this parameter regime.

We remark that a single transition rate in the population dynamics means that the activation and relaxation rates are equal, which is only possible in the high temperature regime as those bath-specific rates satisfy the detailed balance relation.¹⁸ In this regime, the memory of the system is totally destroyed by environments. Therefore, we find the white noise spectrum for the FDCN in the NESB model. It is desirable to investigate the FDCN in systems consisting of multi-states; for such setups, interference effects play an important role in transition rates at strong system-bath couplings⁵³ which may change the behaviors of the FDCN.

B. Effect of bias

In the presence of bias, we still focus on the two coupling strength limits. The numerical results based on the χ -dependent NE-PTRE [Eq. (36)] are shown in Fig. 5. In the weak coupling regime with $\alpha = 0.05$ [Fig. 5(a)], behaviors of $S(\omega)$ as a function of ω with nonzero bias are similar to those with zero bias in Fig. 3(a) and the FDCN increases as the bias increases, implying that fluctuations are more prominent with larger bias in this regime.

For weak couplings, we can use the energy basis of the two level system. Nonzero bias will change the energy gap from Δ to ω_0 with the system Hamiltonian reading $H_s = \omega_0 \sigma_z/2$. The original interaction term becomes

$$H_I = \sum_v (\sigma_z \cos \theta - \sigma_x \sin \theta) \otimes B_v \quad (51)$$

with B_v given by Eq. (28) and $\theta = \tan^{-1}(\Delta/\omega_0)$. It is evident that only the σ_x component in the interaction term contributes to spin-flip processes and thus to heat transfer in the Redfield picture. This implies that the transition rate k_v defined in Eq. (38) should be replaced by $\sin^2 \theta k_v$ in the presence of nonzero bias.¹³ Therefore, if we make the following replacements in Eqs. (42) and (43),

$$\Delta \rightarrow \omega_0, \quad R \rightarrow \sin^2 \theta R, \quad D \rightarrow \sin^2 \theta D, \quad (52)$$

then the universal relation Eq. (44) can still be applied to nonzero bias situations, as confirmed by our numerical results presented in the inset of Fig. 5(a).

However, for strong couplings, nonzero bias leads to totally distinct behaviors compared with the zero bias case. As can be seen from the inset of Fig. 5(b), now $S(\omega)$ is no longer a white noise spectrum and is suppressed by the bias, in direct contrast to its zero frequency counterpart which is insensitive to the bias change.²⁰ To understand the role of finite bias in the strong coupling limit, we note that the χ -dependent Liouvillian operator in the NE-NIBA framework now becomes^{18,19,49}

$$\mathbb{L}_\chi^N = \begin{pmatrix} K(\varepsilon_0) & -K_\chi(-\varepsilon_0) \\ -K_\chi(\varepsilon_0) & K(-\varepsilon_0) \end{pmatrix}, \quad (53)$$

where $K_\chi(\pm\varepsilon_0) = (\eta\Delta/2)^2 \int_{-\infty}^{\infty} dt e^{\pm i\varepsilon_0 t + Q_L(t-\chi) + Q_R(t)}$ and $K(\pm\varepsilon_0) = K_\chi(\pm\varepsilon_0)|_{\chi=0}$ are transfer rates.

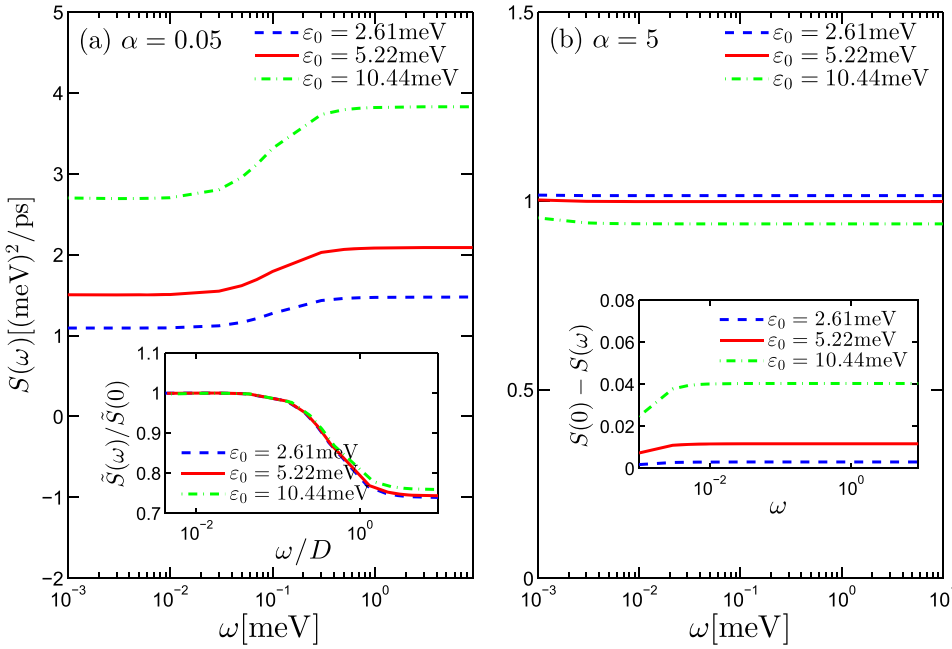


FIG. 5. Behaviors of noise spectrum $S(\omega)$ as a function of ω with varying bias ε_0 for (a) $\alpha = 0.05$ and (b) $\alpha = 5$. The inset in (a) shows universal behaviors of a scaled noise power $\tilde{S}(\omega)$ defined in Eq. (43) with scale parameters given by Eq. (52) in the weak coupling regime and the inset in (b) presents the deviation of $S(\omega)$ from $\tilde{S}(0)$ as a function of ω . Other parameters are $\Delta = 5.22$ meV, $\omega_c = 26.1$ meV, $T_L = 180$ K, and $T_R = 90$ K.

By diagonalizing \mathbb{L}_χ^N , we find $\mu_0(\chi) = \frac{1}{2}[\Xi(\varepsilon_0) - \Xi_\chi(\varepsilon_0)]$ and $\mu_1(\chi) = \frac{1}{2}[\Xi(\varepsilon_0) + \Xi_\chi(\varepsilon_0)]$, where we denote $\Xi(\varepsilon_0) \equiv K(\varepsilon_0) + K(-\varepsilon_0)$ and $\Xi_\chi(\varepsilon_0) \equiv \sqrt{(K(\varepsilon_0) - K(-\varepsilon_0))^2 + 4K_\chi(-\varepsilon_0)K_\chi(\varepsilon_0)}$; the corresponding eigenvectors read

$$\begin{aligned} \langle\langle g_n(\chi) | \rangle\rangle &= \frac{(K_\chi(\varepsilon_0), K(\varepsilon_0) - \mu_n(\chi))}{K_\chi(-\varepsilon_0)K_\chi(\varepsilon_0) + (K(\varepsilon_0) - \mu_n(\chi))^2}, \\ |f_n(\chi)\rangle\rangle &= (K_\chi(-\varepsilon_0), K(\varepsilon_0) - \mu_n(\chi))^T. \end{aligned} \quad (54)$$

Since $\langle\langle g_1(\chi) | \rho_s^{stat} \rangle\rangle \neq 0$ and $\langle\langle \tilde{0} | f_1(\chi) \rangle\rangle \neq 0$, the resulting MGF obviously no longer equals $e^{-\mu_0(\chi)t}$ as it contains a contribution from the eigenvalue $\mu_1(\chi)$ according to Eq. (20); thus

we expect the frequency dependence of $S(\omega)$ in the presence of bias, as Fig. 5(b) shows.

C. Effect of temperature difference

Now we extend our analysis of FDCN to the impact of temperature difference ranging from the linear response regime to the nonlinear situation.

1. $\omega = 0$: Thermodynamic consistency

In the zero frequency limit, the NESB model we consider satisfies the Gallavotti-Cohen (GC) symmetry,⁵⁴ as shown in previous studies;^{19,50} thus, the Saito-Utsumi (SU) relations can be applied to $J_m^n = \lim_{t \rightarrow \infty} \frac{\partial}{\partial t} C_m^n(t)$ [see Eq. (22)], yielding⁵⁵

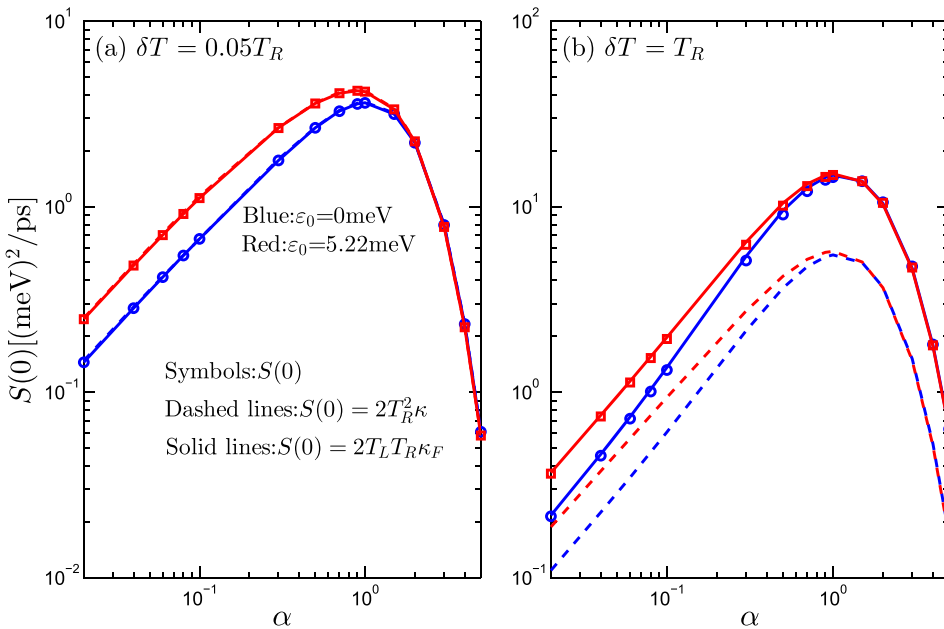


FIG. 6. Behaviors of noise spectrum $S(0)$ as a function of α with varying bias for (a) temperature difference $\delta T = 0.05T_R$ and (b) $\delta T = T_R$. Symbols are direct results of $S(0)$, using our theory, dashed lines are predictions of Eq. (57), and solid lines are predictions of Eq. (56). Other parameters are $\Delta = 5.22$ meV, $\omega_c = 26.1$ meV, $T_L = T_R + \delta T$, and $T_R = 90$ K.

$$J_m^n = \sum_{l=0}^m \binom{m}{l} (-1)^{n+l} J_{m-l}^{n+l}, \quad (55)$$

from which we find $2J_1^1 = J_0^2$ and thus $S(0) = 2\frac{\partial I_L}{\partial A}$ by noting $S(0) = J_0^2$. Associated with the coefficient J_1^1 , we can introduce a first-order energetic transport coefficient as³² $\kappa_F \equiv \beta_L \beta_R J_1^1$; therefore,

$$S(0) = 2T_L T_R \kappa_F. \quad (56)$$

For small temperature differences, Eq. (56) reduces to a linear response relation²⁴

$$S(0) = 2T^2 \kappa \quad (57)$$

with κ being the heat conductance. For later purposes, first we check that our theory indeed satisfies Eq. (56) and thus preserves the GC symmetry in the zero frequency limit. As shown in Fig. 6, we clearly see good agreements between numerical results and theoretical relations. Equation (57) captures the behaviors of $S(0)$ with small temperature differences in the entire coupling strength range regardless of values of bias, while Eq. (56) holds generally in our theory regardless of the magnitude of the temperature difference.

2. Frequency dependence

Now we investigate $S(\omega)$. So far, there are no general relations between $S(\omega)$ and first order quantities characterizing the response to arbitrary temperature difference for finite frequency cases.²⁴ However, according to above universal behaviors in the two coupling strength limits, we can formulate general relations valid in the corresponding coupling strength regimes. The white noise behavior in the strong coupling regime for unbiased systems implies that the SU relation Eq. (56) can be directly applied to the FDCN, namely,

$$S(\omega) = 2T_L T_R \kappa_F. \quad (58)$$

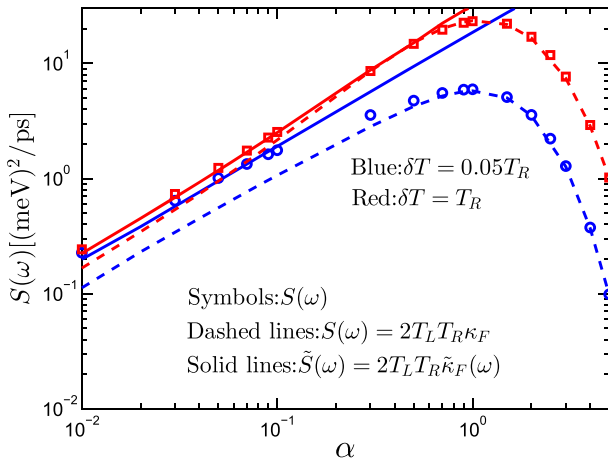


FIG. 7. Behaviors of noise spectrum $S(\omega)$ as a function of α with varying temperature differences and fixed $\omega = 0.5$. Blue color denotes $\delta T = 0.05T_R$ and red color denotes $\delta T = T_R$. Symbols are direct numerical results of $S(\omega)$ based on the χ -dependent NE-PTRE, Eq. (36), dashed lines are predictions of a strong coupling relation, Eq. (58), and solid lines are predictions of a weak coupling expression Eq. (59). Other parameters are $\Delta = 5.22$ meV, $\omega_c = 26.1$ meV, $\varepsilon_0 = 0$ meV. $T_L = T_R + \delta T$, and $T_R = 90$ K.

While in the weak coupling regime, the universal scaling form Eq. (44) guarantees the following relation:

$$\tilde{S}(\omega) = 2T_L T_R \tilde{\kappa}_F(\omega) \quad (59)$$

for the scaled FDCN $\tilde{S}(\omega)$ and a frequency-dependent first order coefficient $\tilde{\kappa}_F(\omega) = \mathcal{P}(\omega/D) \left[\kappa_F - \frac{\Delta^2 R}{2T_L T_R} \right]$. Their validity can be seen from comparisons in Fig. 7. We find that the weak coupling expression Eq. (59) predicts a monotonically increasing behavior of $S(\omega)$ as a function of α , thus becomes invalid in the intermediate as well as strong coupling regimes. The strong coupling expression Eq. (58) underestimates the current fluctuations in the weak coupling regime. Although our theory can provide a detailed description for the FDCN with arbitrary temperature differences in the two limits of coupling strength, a general yet simple relation for $S(\omega)$ and temperature differences beyond these two coupling limits is desirable and will be addressed in the future studies.

V. SUMMARY

We formulate a general theory to study the frequency-dependent current noise (FDCN) in open quantum systems at steady states. To go beyond previous results, we extend MacDonald's formula from electron transport to heat current and obtain a formally exact relation which relates the FDCN to the time-dependent second order cumulant of heat evaluated at steady states. In order to calculate the time-dependent cumulant of heat involved in the FDCN, we follow the scheme of a finite time full counting statistics (FCS) developed for electron transport and propose an analogous framework, which can be applied to open quantum systems described by Markovian quantum master equations.

To demonstrate the utility of the approach, we consider the nonequilibrium spin-boson model which is a paradigmatic example of quantum heat transfer. A recently developed polaron-transformed Redfield equation for the reduced spin dynamics enables us to study the FDCN from weak to strong system-reservoir coupling regimes and consider arbitrary values of bias and temperature differences. Key findings are as follows:

- (1) By varying coupling strengths, we observe a turn-over behavior for the FDCN in moderate coupling regimes, similar to the zero frequency counterpart. Interestingly, the FDCN with varying coupling strength or bias exhibits a universal Lorentzian-shape scaling form in the weak coupling regime as confirmed by numerical results as well as analytical analysis, while it becomes a white noise spectrum under the condition of strong coupling strengths and zero bias. The white noise spectrum is distorted in the presence of a finite bias.
- (2) We also find that the bias can suppress frequency-dependent current fluctuations in the strong coupling regime, in direct contrast to the zero frequency counterpart which is insensitive to the bias changes.
- (3) We further utilize the Saito-Utsumi (SU) relation as a benchmark to evaluate the theory at the zero frequency limit in the entire coupling range. Agreements between

the SU relation and our zero frequency results show that our theory preserves the Gallavotti-Cohen symmetry. Noting the universal behaviors of the FDCN in the weak as well as strong coupling regimes, we then study the impact of temperature differences at finite frequencies by carefully generalizing the SU relations. Our results thus provide detailed dissections and a unified framework for studying the finite time fluctuation of heat in open quantum systems.

ACKNOWLEDGMENTS

J. Liu thanks Chen Wang for correspondences on related topics and Michael Moskalets for interesting comments. The authors acknowledge the support from the Singapore-MIT Alliance for Research and Technology (SMART).

APPENDIX: MACDONALD-LIKE FORMULA FOR HEAT TRANSFER

Here, we would like to present the derivation of MacDonald's formula for heat transfer. Noting that in the Heisenberg picture $Q(t) = H_B^L(t) - H_B^L(0)$, we have

$$\int_0^t \Delta I(t') dt' = Q(t) - \langle Q(t) \rangle. \quad (\text{A1})$$

Using the expectation value of the square of the above expression, the inverse Fourier transform and setting $t = t' - t''$, we find

$$\begin{aligned} 2\langle Q^2(t) \rangle_c &\equiv 2\langle [Q(t) - \langle Q(t) \rangle]^2 \rangle \\ &= \left\langle \int_0^t \int_0^t [\Delta I(t') \Delta I(t'') + \Delta I(t'') \Delta I(t')] dt' dt'' \right\rangle \\ &= \int_0^t \int_0^t dt' dt'' \int_{-\infty}^{\infty} \frac{1}{\pi} S(\omega) e^{i\omega(t'-t'')} d\omega, \end{aligned} \quad (\text{A2})$$

where we have introduced the second order cumulant of $Q(t)$ as $\langle Q^2(t) \rangle_c$. Rearranging and performing the time integrals we obtain

$$\begin{aligned} 2\langle Q^2(t) \rangle_c &= \int_{-\infty}^{\infty} \frac{1}{\pi} S(\omega) \frac{1}{\omega^2} (e^{-i\omega t} - 1)(e^{i\omega t} - 1) d\omega \\ &= \frac{2}{\pi} \int_{-\infty}^{\infty} S(\omega) \frac{1}{\omega^2} (1 - \cos \omega t) d\omega. \end{aligned} \quad (\text{A3})$$

Differentiating both sides with respect to t gives

$$\frac{\partial}{\partial t} \langle Q^2(t) \rangle_c = \frac{1}{\pi} \int_{-\infty}^{\infty} \frac{S(\omega)}{\omega} \sin \omega t d\omega \quad (\text{A4})$$

and performing the Fourier transform with $\int_{-\infty}^{\infty} e^{i\omega' t} dt$,

$$\begin{aligned} \int_{-\infty}^{\infty} e^{i\omega' t} dt \frac{\partial}{\partial t} \langle Q^2(t) \rangle_c &= \frac{1}{\pi} \int_{-\infty}^{\infty} \int_{-\infty}^{\infty} \frac{S(\omega)}{\omega} \sin \omega t e^{i\omega' t} dt d\omega \\ &= \frac{2i}{\omega'} S(\omega'). \end{aligned} \quad (\text{A5})$$

We can match the odd and imaginary parts of the above equation to give (and setting $\omega = \omega'$)

$$\int_{-\infty}^{\infty} \sin \omega t \frac{\partial}{\partial t} \langle Q^2(t) \rangle_c dt = \frac{2}{\omega} S(\omega). \quad (\text{A6})$$

Again using the fact that $S(\omega) = S(-\omega)$ and that the original correlator is symmetric in t implies that the integral over t can be written as

$$S(\omega) = \omega \int_0^{\infty} dt \sin \omega t \frac{\partial}{\partial t} \langle Q^2(t) \rangle_c, \quad (\text{A7})$$

which is just Eq. (5) in the main text.

- ¹W. Lee, K. Kim, W. Jeong, L. A. Zotti, F. Pauly, J. C. Cuevas, and P. Reddy, *Nature* **498**, 209 (2013).
- ²S. Jezouin, F. D. Parmentier, A. Anthore, U. Gennser, A. Ca-vanna, Y. Jin, and F. Pierre, *Science* **342**, 601 (2013).
- ³J. Ankerhold, *Phys. Rev. Lett.* **98**, 036601 (2007).
- ⁴M. A. Ochoa, Y. Selzer, U. Peskin, and M. Galperin, *J. Phys. Chem. Lett.* **6**, 470 (2015).
- ⁵F. Battista, M. Moskalets, M. Albert, and P. Samuelsson, *Phys. Rev. Lett.* **110**, 126602 (2013).
- ⁶H. Touchette, *Phys. Rep.* **478**, 1 (2009).
- ⁷C. Jarzynski and D. K. Wójcik, *Phys. Rev. Lett.* **92**, 230602 (2004).
- ⁸M. Esposito, U. Harbola, and S. Mukamel, *Rev. Mod. Phys.* **81**, 1665 (2009).
- ⁹U. Seifert, *Rep. Prog. Phys.* **75**, 126001 (2012).
- ¹⁰L. S. Levitov and G. B. Lesovik, *Pisma Zh. Eksp. Teor. Fiz.* **58**, 225 (1993).
- ¹¹D. A. Bagrets and Y. V. Nazarov, *Phys. Rev. B* **67**, 085316 (2003).
- ¹²B. K. Agarwalla, B. Li, and J.-S. Wang, *Phys. Rev. E* **85**, 051142 (2012).
- ¹³N. Boudjada and D. Segal, *J. Phys. Chem. A* **118**, 11323 (2014).
- ¹⁴C. Wang, J. Ren, and J. Cao, *Sci. Rep.* **5**, 11787 (2015).
- ¹⁵J. Liu, H. Xu, B. Li, and C. Wu, *Phys. Rev. E* **96**, 012135 (2017).
- ¹⁶K. Saito and A. Dhar, *Phys. Rev. Lett.* **99**, 180601 (2017).
- ¹⁷U. Peskin, *J. Phys. B: At., Mol. Opt. Phys.* **43**, 153001 (2010).
- ¹⁸L. Nicolin and D. Segal, *J. Chem. Phys.* **135**, 164106 (2011).
- ¹⁹L. Nicolin and D. Segal, *Phys. Rev. B* **84**, 161414 (2011).
- ²⁰C. Wang, J. Ren, and J. Cao, *Phys. Rev. A* **95**, 023610 (2017).
- ²¹B. K. Agarwalla and D. Segal, *New J. Phys.* **19**, 043030 (2017).
- ²²F. Zhan, S. Denisov, and P. Hänggi, *Phys. Rev. B* **84**, 195117 (2011).
- ²³I. V. Krive, E. N. Bogachev, A. G. Scherbakov, and U. Landman, *Phys. Rev. B* **64**, 233304 (2001).
- ²⁴D. V. Averin and J. P. Pekola, *Phys. Rev. Lett.* **104**, 220601 (2010).
- ²⁵H.-P. Breuer and F. Petruccione, *The Theory of Open Quantum Systems* (Oxford University Press, Oxford, 2007).
- ²⁶U. Weiss, *Quantum Dissipative Systems* (World Scientific, Singapore, 2012).
- ²⁷G. Schaller, *Open Quantum Systems Far from Equilibrium* (Springer, Heidelberg, 2014).
- ²⁸D. K. C. MacDonald, *Rep. Prog. Phys.* **12**, 56 (1949).
- ²⁹N. Lambert, R. Aguado, and T. Brandes, *Phys. Rev. B* **75**, 045340 (2007).
- ³⁰C. Emary, D. Marcos, R. Aguado, and T. Brandes, *Phys. Rev. B* **76**, 161404(R) (2007).
- ³¹D. Marcos, C. Emary, T. Brandes, and R. Aguado, *New J. Phys.* **12**, 123009 (2010).
- ³²J. Cerrillo, M. Buser, and T. Brandes, *Phys. Rev. B* **94**, 214308 (2016).
- ³³A. J. Leggett, S. Chakravarty, A. T. Dorsey, M. P. A. Fisher, A. Garg, and W. Zwerger, *Rev. Mod. Phys.* **59**, 1 (1987).
- ³⁴C. Wang, J. Ren, and J. Cao, *New J. Phys.* **16**, 045019 (2014).
- ³⁵D. Xu, C. Wang, Y. Zhao, and J. Cao, *New J. Phys.* **18**, 023003 (2016).
- ³⁶J. Thingna, D. Manzano, and J. Cao, *Sci. Rep.* **6**, 28027 (2016).
- ³⁷M. Esposito, M. A. Ochoa, and M. Galperin, *Phys. Rev. Lett.* **114**, 080602 (2015).
- ³⁸C. Flindt, T. Novotný, and A.-P. Jauho, *Phys. E* **29**, 411 (2005).
- ³⁹M. Campisi, P. Hänggi, and P. Talkner, *Rev. Mod. Phys.* **83**, 771 (2011).
- ⁴⁰A. Braggio, J. Koenig, and R. Fazio, *Phys. Rev. Lett.* **96**, 026805 (2006).
- ⁴¹C. Flindt, T. Novotný, A. Braggio, M. Sassetti, and A.-P. Jauho, *Phys. Rev. Lett.* **100**, 150601 (2008).
- ⁴²D. Marcos, C. Emary, T. Brandes, and R. Aguado, *Phys. Rev. B* **83**, 125426 (2011).
- ⁴³R. J. Cook, *Phys. Rev. A* **23**, 1243 (1981).
- ⁴⁴S. A. Gurvitz, *Phys. Rev. B* **57**, 6602 (1998).
- ⁴⁵R. Görlich, M. Sassetti, and U. Weiss, *Europhys. Lett.* **10**, 507 (1989).
- ⁴⁶C. K. Lee, J. Moix, and J. Cao, *J. Chem. Phys.* **136**, 204120 (2012).

- ⁴⁷J. Liu, H. Xu, and C. Wu, *Chem. Phys.* **481**, 42 (2016).
- ⁴⁸D. Segal, *Phys. Rev. B* **73**, 205415 (2006).
- ⁴⁹T. Chen, X.-B. Wang, and J. Ren, *Phys. Rev. B* **87**, 144303 (2013).
- ⁵⁰J. Ren, P. Hänggi, and B. Li, *Phys. Rev. Lett.* **104**, 170601 (2010).
- ⁵¹C. Maes and M. H. van Wieren, *Phys. Rev. Lett.* **96**, 240601 (2006).
- ⁵²V. Lecomte, C. Appert-Rolland, and F. van Willand, *J. Stat. Phys.* **127**, 51 (2007).
- ⁵³S. Jang and J. Cao, *J. Chem. Phys.* **114**, 9959 (2001).
- ⁵⁴G. Gallavotti and E. G. D. Cohen, *Phys. Rev. Lett.* **74**, 2694 (1995).
- ⁵⁵K. Saito and Y. Utsumi, *Phys. Rev. B* **78**, 115429 (2008).